ASSIMILATION OF SINGLE LEVEL WIND DATA

A.C. Lorenc
U.K. Meteorological Office

Summary: An example of the impact of aircraft wind data on the Meteorological Office FGGE data assimilation scheme is presented, and the behaviour is explained using simple models based on linear geostrophic adjustment theory.

1. INTRODUCTION

This study was prompted by an observing system experiment to evaluate the impact of aircraft wind data (Lorenc 1982). In this experiment several cases were found where aircraft data had a significant impact on the wind analyses, particularly at jet level over the Northern Hemisphere oceans. Although some improvements downstream were noticed during the subsequent forecasts, much of the analysis improvement seemed to be lost during the early stages of the forecasts, whereas this information loss was less evident in a similar OSE conducted at ECMWF. One example was studied in detail to try to understand the cause of this.

2. AN EXAMPLE FROM THE AIRCRAFT WIND OSE

Figure 1 shows the with-aircraft analysis for the North Pacific, with the aircraft observation of interest enlarged. (Actually there were two similar collocated observations). Isotachs are shown dotted, labelled in metres per second, and on the observations each full fleche =5 m/s. Figure 2 shows the corresponding without-aircraft analysis; it is clear that the aircraft data have caused a large increase in jet speed. In the forecasts from these analyses this difference decreases, although it remains of correct sign (i.e. the forecast from the with-aircraft analysis is better) during the next 3 days, as shown by the sequence of difference maps on the left of figure 3.

The ECMWF with-aircraft analysis (figure 4) was similar to ours, as was the difference between their with- and without-aircraft analyses (figure 3 top right). However during their forecast this information was retained better.

A study of our forecasts (figures 5 and 6) shows that much of this information loss occurs in 6 hours. In order to confirm that this is due to our analyses rather than our forecast model, a forecast was made with our model from the ECMWF with-aircraft analysis. This retains the jet maximum (figure 7), and is probably more nearly correct, although its similarity to the verifying ECMWF analysis (figure 8) is not conclusive proof of this since there are few data.

3. DATA-ASSIMILATION TECHNIQUE

This was based on the data-assimilation scheme used to produce near real time analysis for general circulation studies during the FGGE special observing periods (Lyne et al 1982), and an 11-layer general circulation model (Saker 1975). The assimilation method was repeated interpolation and insertion into the model; at each time-step for a 6-hour period, pressure, temperature, wind and humidity data were interpolated univariately and horizontally to the model's grid, using a one time-step forecast from the previous estimate as first-guess, and giving steadily increasing weight to the observations. The resolution of the model was about 220 km and 80 mb in the upper troposphere. Details of modifications to the Lyne et al (1981) version are given by Barwell (1982).

Although similar in principle and some details to the suite recently brought into operational use at the Meteorological Office, this suite has not been subjected to the intensive testing and development given to the operational one, and differs in some significant details such as the lack of vertical coupling.

Unlike ours, the ECMWF data assimilation system attempts explicitly to maintain a balance between mass and wind fields by doing a multivariate analysis (Lorenc 1981) and incorporating a non-linear normal mode initialization step (Temperton and Williamson 1981). It also uses single level data three-dimensionally rather than only at the nearest level as our system does.

4. LINEARIZED GEOSTROPHIC ADJUSTMENT THEORY

Let us express perturbations to the forecast "first-guess" in terms of rotational wind defined by streamfunction ψ and divergent wind defined by velocity potential χ and mass field defined by geopotential ϕ. If we linearize, and treat vertical modes (chatacterized by equivalent depth Φ) and horizontal scales (characterized by wavelength λ) separately, then geostrophic adjustment theory (Temperton 1973) can be used. This states that, assuming divergent (gravity wave) modes disperse and are damped

$$\psi_{final} = \psi_{initial} + (1 - \alpha)\ \psi_{initial\ geostrophic}$$
$$\alpha = (1 + f^2 \lambda^2 / 4\pi^2 \Phi)^{-1} \qquad (1)$$

The difference fields between our with- and without-aircraft analyses and forecasts can be studied in these terms. That the analysis differences are indeed ageostrophic can be seen in figure 9, which shows that the wind difference and its ageostrophic component are almost equal. 6 hours later some adjustment has taken place, with the main wind difference advected, veered through about 90°, and decreased in magnitude (figure 10). The more nearly geostrophic difference in the original position is much smaller than it was for the analyses.

Only about $\frac{2}{3}$ of the wind maximum we are studying was rotational (figure 11), the rest being divergent and hence dispersed and damped in this simple theory. Studies of analysis difference charts at other levels or of vertical cross sections (see Lorenc 1982) show that there is an opposite flow at adjacent levels. Thus much of the analysis impact is on the highest order internal vertical modes, with equivalent depth less than about 10 m. From figure 9 we can estimate a wavelength of between 1500 and 3000 km. For this scale, equivalent depth and latitude the geostrophic adjustment theory states that only about 5 to 15% of the original wind impact will be retained.

5. MODEL PERTURBATION EXPERIMENTS

To isolate the effect of different analysis techniques and confirm the applicability of the above theory to multi-level primitive equation models, we performed a series of 4 perturbation experiments, adding idealized increments to a balanced state selected from a general circulation integration. The example of section 4 was simulated by adding a zonal wind component increment (figure 12) to a straight zonal jet at the level of maximum wind (232 mb), altering one sigma layer of the model only. The difference between forecasts from this and the unperturbed field was studied; after 6 hours the perturbation has advected, veered through about 90°, and decreased (figure 13), in a very similar manner to that shown in figure 10. There is a large outward propagating gravity wave which returns after a great circle path round the earth after 38 hours, implying an equivalent depth of 8730 m.

A better analysis scheme would spread vertically the effect of any observation, although how much spreading is optimum is uncertain. We tested the effect of a rather small vertical coupling, in fact that in the current operational Meteorological Office analysis, by adding the perturbation of figure 12 to all nearby levels with weights given by $\exp(-3 \log^2(p/p_{obs}))$. We estimate that this profile projects mainly on vertical modes with equivalent depth between 20 m and 200 m. This multi-level perturbation behaved qualitatively similarly to the single level one. In the 6 hour forecast (figure 14) wind speeds are smaller, the low and high more intense, and the external gravity wave stronger.

If we assume that for this type of situation most of the error in the first-guess is in rotational modes, then observational information should be used to change these rather than divergent modes. Formulae for doing this are given by Lorenc (1981), and the corresponding perturbations for height and wind shown in figure 15. A forecast from this wind perturbation with vertical structure as in the multi-level experiment showed a markedly different impact after 6 hours (figure 16). The main wind perturbation has remained approximately zonal, appropriate highs and lows have developed in the height field to balance the winds, the external gravity wave

is much smaller, and there are some internal (slower propagating) gravity waves generated by the geostrophic adjustment in the main low and high.

Finally we tested the full geostrophic increment (mass and wind fields) of figure 15. The 6 hour forecast is shown in figure 17. It is qualitatively similar to that from the rotational perturbation, but the central features are more intense and the propagating gravity waves less.

The mean square impact on the rotational wind is plotted against time in figure 24 for all four experiments, for the area of figure 13. The single-level experiment's curve drops slowest, because the gravity wave propagation speed ($\sqrt{g\bar{\Phi}}$) is least, but the final impact is least and in approximate agreement with the theory of section 4. The multi-level experiment levels off at twice the impact of the single-level because of its greater equivalent depth, before increasing again, probably because of developments triggered by the large vertical motions associated with internal gravity waves with larger equivalent depth. The oscillations visible in the rotational and geostrophic experiment have periods consistent with gravity waves of the horizontal scale (wavelength 2000 km) and equivalent depth (200 m) excited. Gravity waves would be excited even for the geostrophic perturbation because the large wind speed and curvature make the geostrophic approximation inaccurate.

6. SIMPLE LINEAR MODEL EXPERIMENTS

The results of the experiments in section 5 justify the use of linear geostrophic adjustment theory to describe the response to isolated wind data. However such experiments are rather cumbersome, and a much simpler model can reproduce the main features quite well, and be used to study the effect of the repeated insertion analysis technique. If we linearize the equations of motion, and assume that the analysis method only excites modes of one equivalent depth and horizontal scale, we are left with a predictive model with only 12 degrees of freedom. Results from such a model simulating the four experiments of section 4 are shown in figures 18-23, which should be compared with figures 12-17. If we concentrate on the evolution of the central wind maxima then the similarity is evident.

This simple model can be used to study the effect of the repeated insertion analysis technique, which mixes the modes and makes an analytic solution very difficult. The behaviour of the real example of section 4 can be simulated (figure 25). We get the maximum impact downstream of the observation, with wind speeds greater than observed and some veering, as in figure 9.

This model can be used to study many aspects of the repeated insertion analysis technique; we give two examples. Repeated insertion selectively excites modes with periods long compared with the insertion period. Thus it is beneficial in

avoiding gravity wave modes only for large equivalent depths. For the wavelength and latitude we have been considering, the energy excited in each mode is shown in figure 26 for univariate insertion as in the Meteorological Office FGGE analysis scheme. This can be compared with the solid curve and crosses of figure 27, which show the same for a single univariate update; repeated insertion is clearly beneficial for larger equivalent depths (high frequencies) but only marginally so for depths less than about 200 m. The dashed curve and triangles in figure 27 show the energies excited by a single update with the non-divergent wind pattern shown in figure 22. For this example such a non-divergent single update is about as effective as repeated insertion done univariately.

The above example is for zero advective wind. If a mean wind is imposed then repeated insertion becomes less effective since the "correct" geostrophic mode then has a finite period. This is illustrated in figure 28, which is for the scale and latitude as figure 26, and an equivalent depth of 200 m. For the wavelength chosen the ordinate is equivalent to advective speed of 0-50 m/s.

7. SUMMARY AND CONCLUSIONS

Forecasts from analyses made with the Meteorological Office FGGE data assimilation scheme fail to retain much of the useful information present in aircraft wind observations; in one case an isolated AIREP had only about half the impact which it had on the ECMWF NWP system. This behaviour can be explained in terms of linear geostrophic adjustment theory. Some simplified perturbation experiments were described which verified the applicability of the theory to a multi-level primitive equation model. A very simple linear model reproduced features of the real analysis and forecast, and was used to study the importance of different aspects of the analysis technique.

Conclusions, valid only for isolated wind observation in extratropical upper tropospheric jets, were:-

(a) It is important to put information in the rotational wind.

(b) Information projected on vertical modes other than those with very small equivalent depth (complex vertical structure) is easier to assimilate. Such a behaviour is anyway a desirable property of analysis schemes in data sparse regions.

(c) Correcting the mass field geostrophically in accordance with the wind observations is less important than (a) and (b), but still has a significant quantitative effect.

(d) Repeated insertion aids the assimilation if (a) and (c) have not been done, by preferentially selecting long period modes.

(e) The presence of a mean advection has a marked detrimental effect on repeated insertion analyses, causing significant changes in the incorrect geostrophic modes.

REFERENCES

Barwell, B.R. 1982 The impact of aircraft data on the Meteorological Office FGGE data assimilation suite: February 1979 case study. Met O 20 Tech. Note No. II/189.

Lorenc, A.C. 1981 A global three-dimensional multivariate statistical analysis scheme. Mon. Wea. Rev. 109, 701-721.

Lorenc, A.C. 1982 The impact of aircraft data on the Meteorological Office FGGE data assimilation suite: November 1979 case study. Met O 20 Tech. Note No. II/190.

Lyne, W.H., Swinbank, R. and Birch, N.T. 1982 A data assimilation experiment and the global circulation during the FGGE special observing periods. Quart. J.R. Met. Soc., 108, 575-594.

Saker, N. 1975 An 11-layer general circulation model. Met O 20 Tech. Note No. II/30.

Temperton, C. 1973 Some experiments in dynamic initialization for a simple primitive equation model. Quart. J.R. Met. Soc., 99, 303-319.

Temperton, C. and Williamson, D.L. 1981 Normal Mode Initialization for a Multi-level Grid-Point Mode. Part 1: Linear Aspects. Mon. Wea. Rev., 109

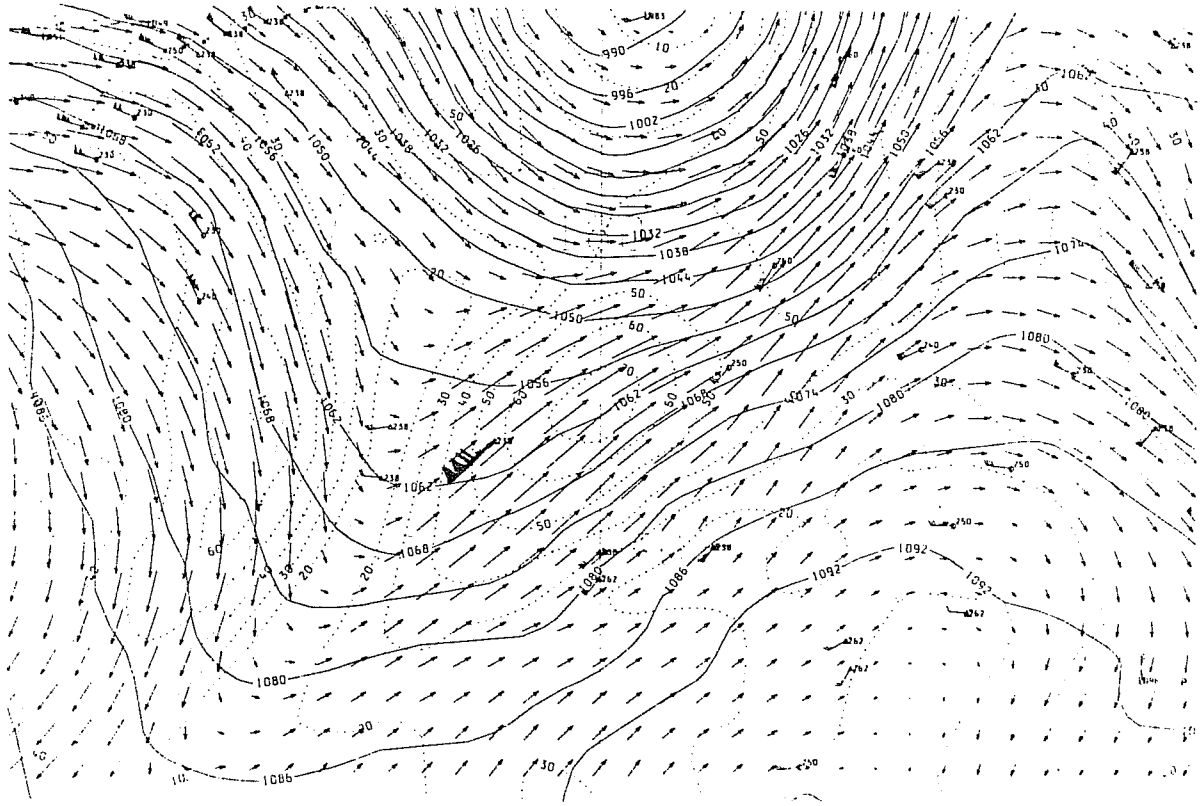

Figure 1. N. Pacific with-aircraft analysis and observations. 250 mb.
00Z 11/11/79.

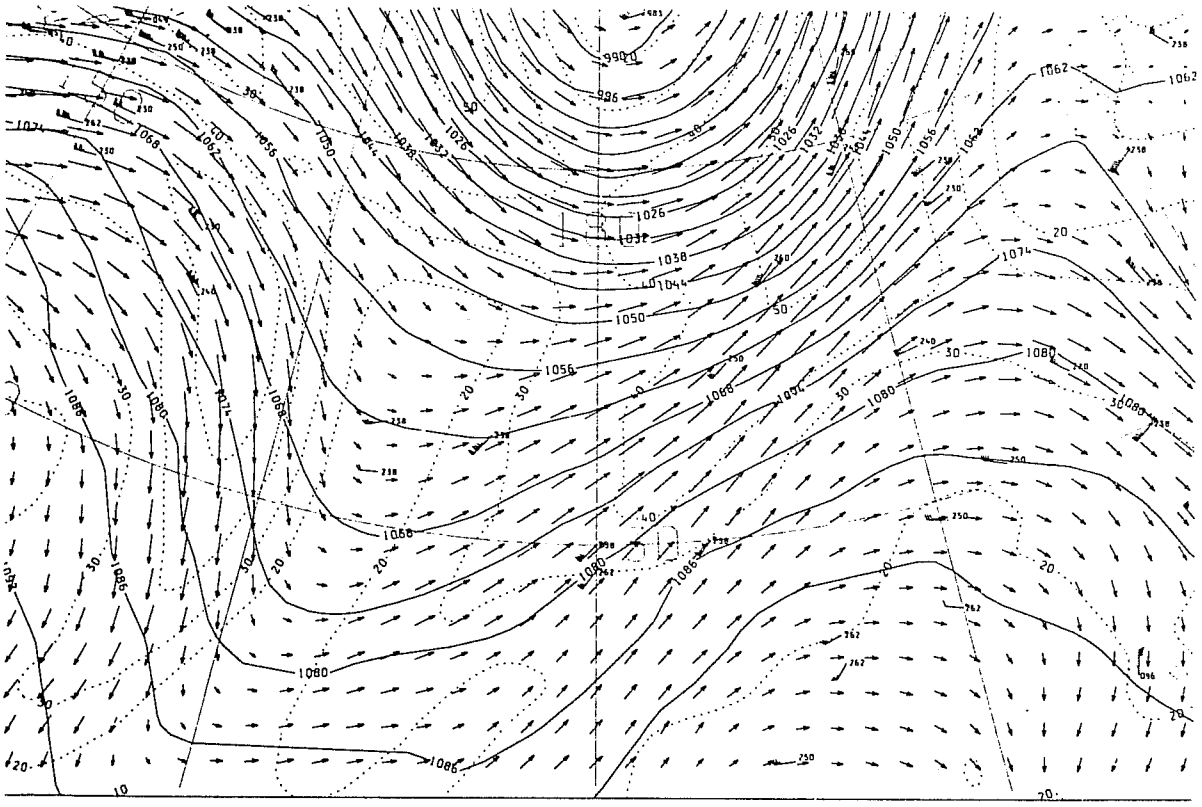

Figure 2 as Figure 1 for without-aircraft analysis.

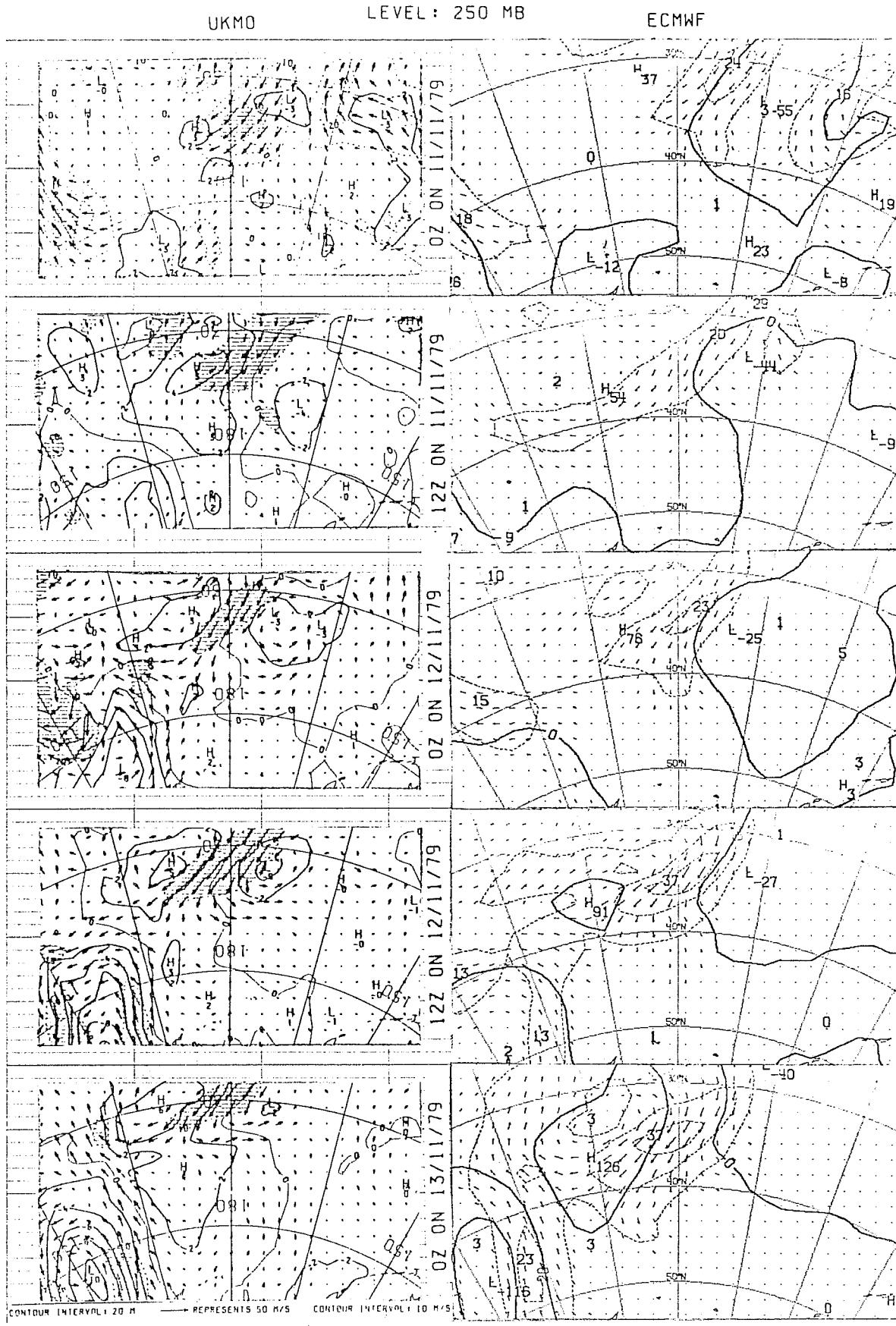

Figure 3. Time sequence showing the evolution of N. Pacific aircraft impact during forecast. Left our experiment. Right ECMWF experiment.

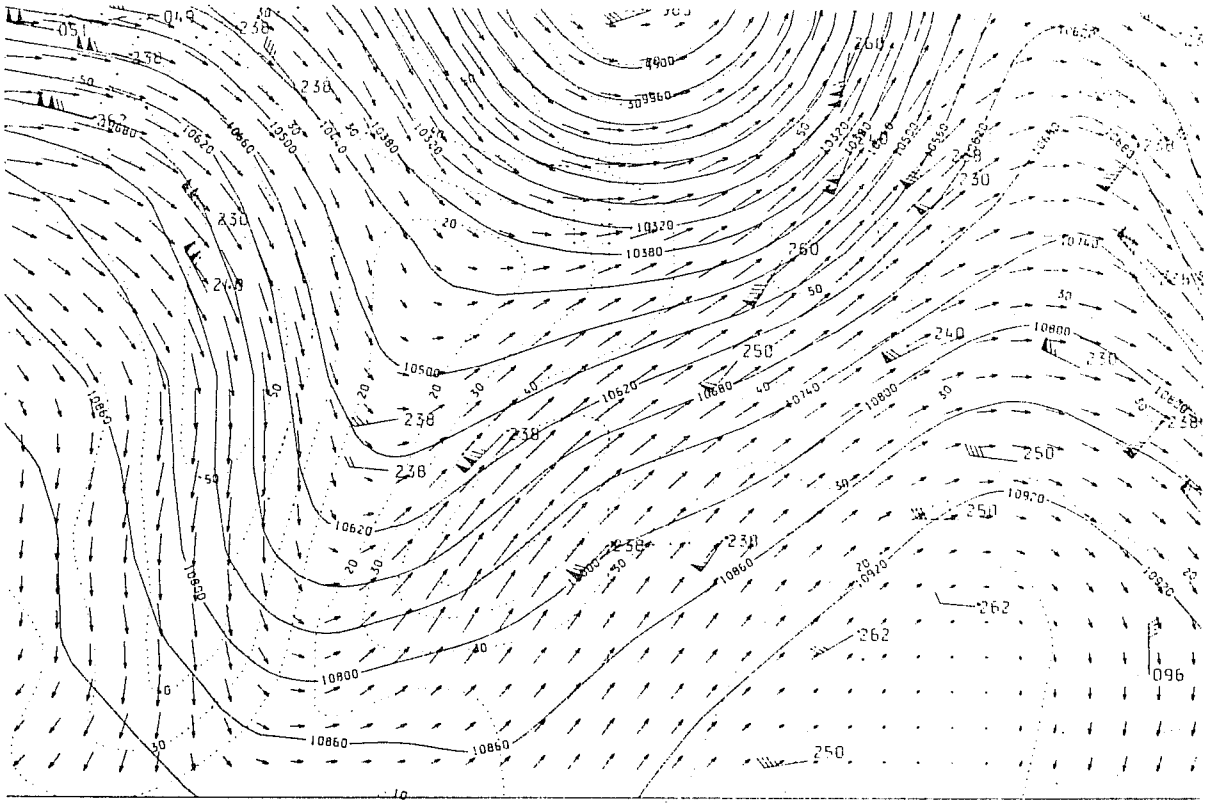

Figure 4 as Figure 1 for ECMWF with-aircraft analysis.

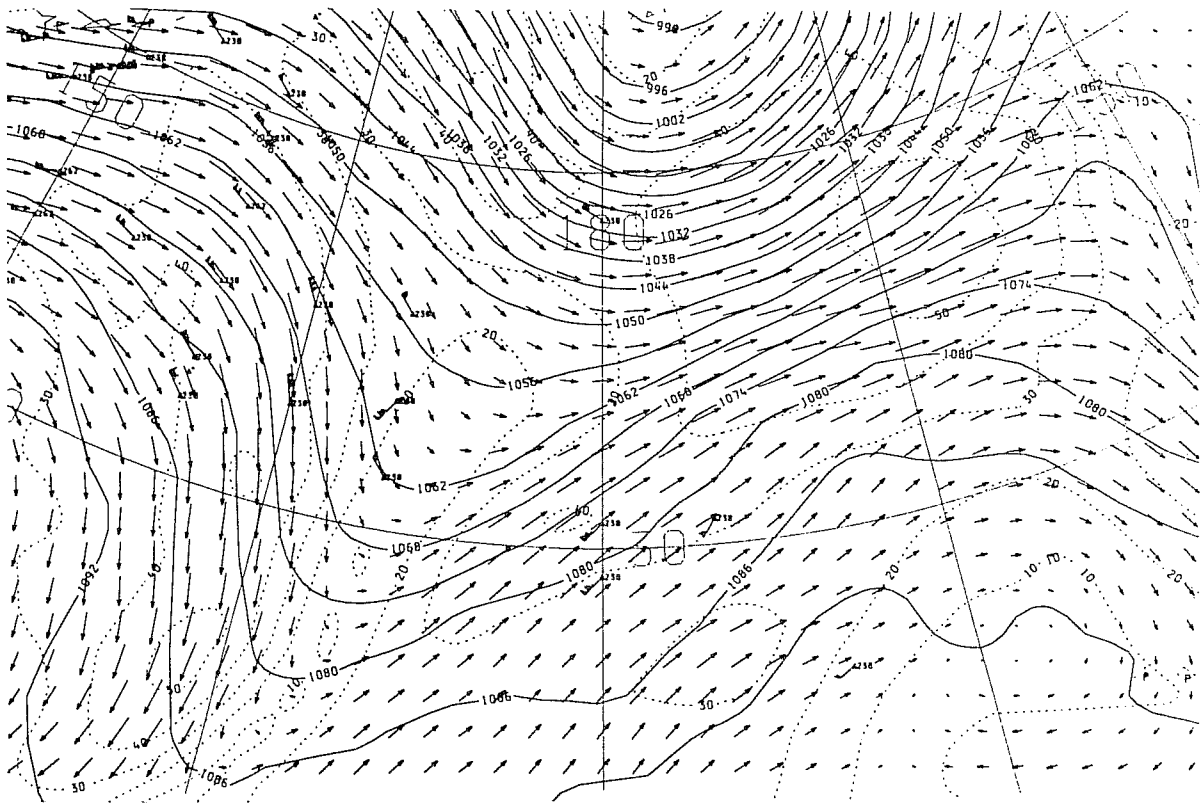

Figure 5. 6 hour forecast from with-aircraft analysis.

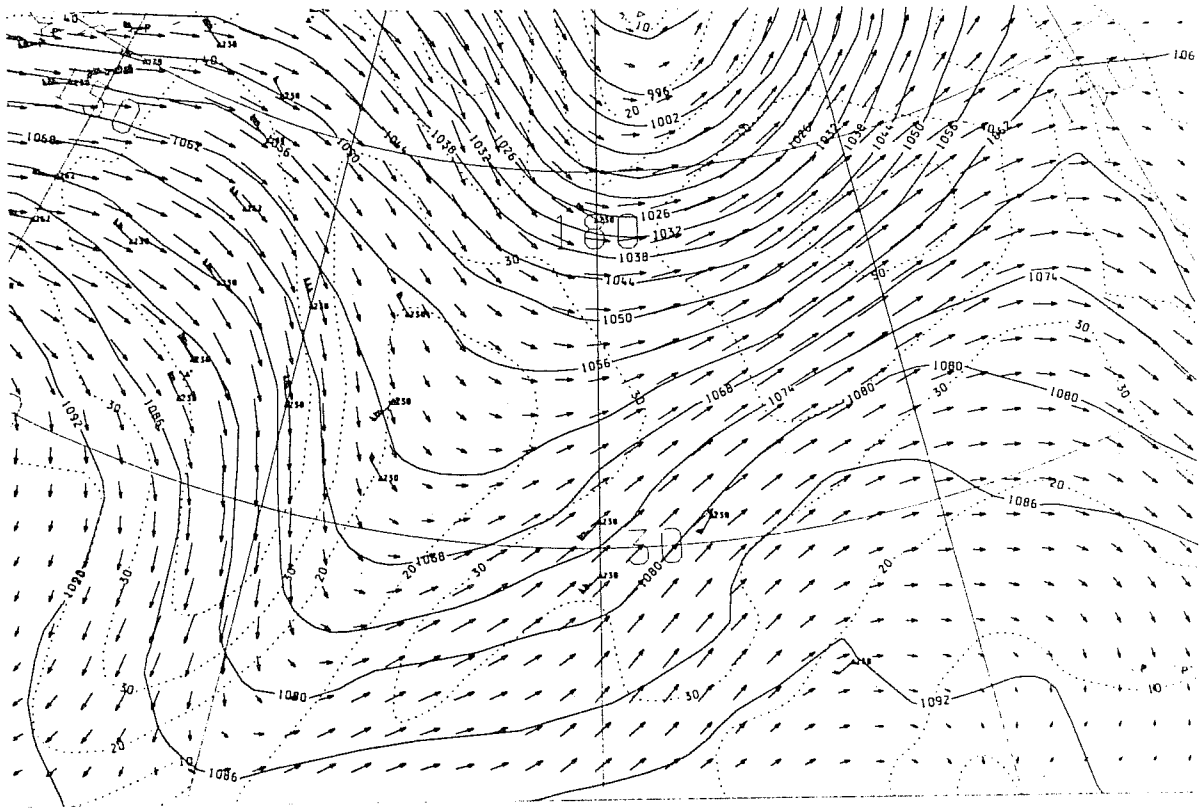

Figure 6. 6 hour forecast from without-aircraft analysis.

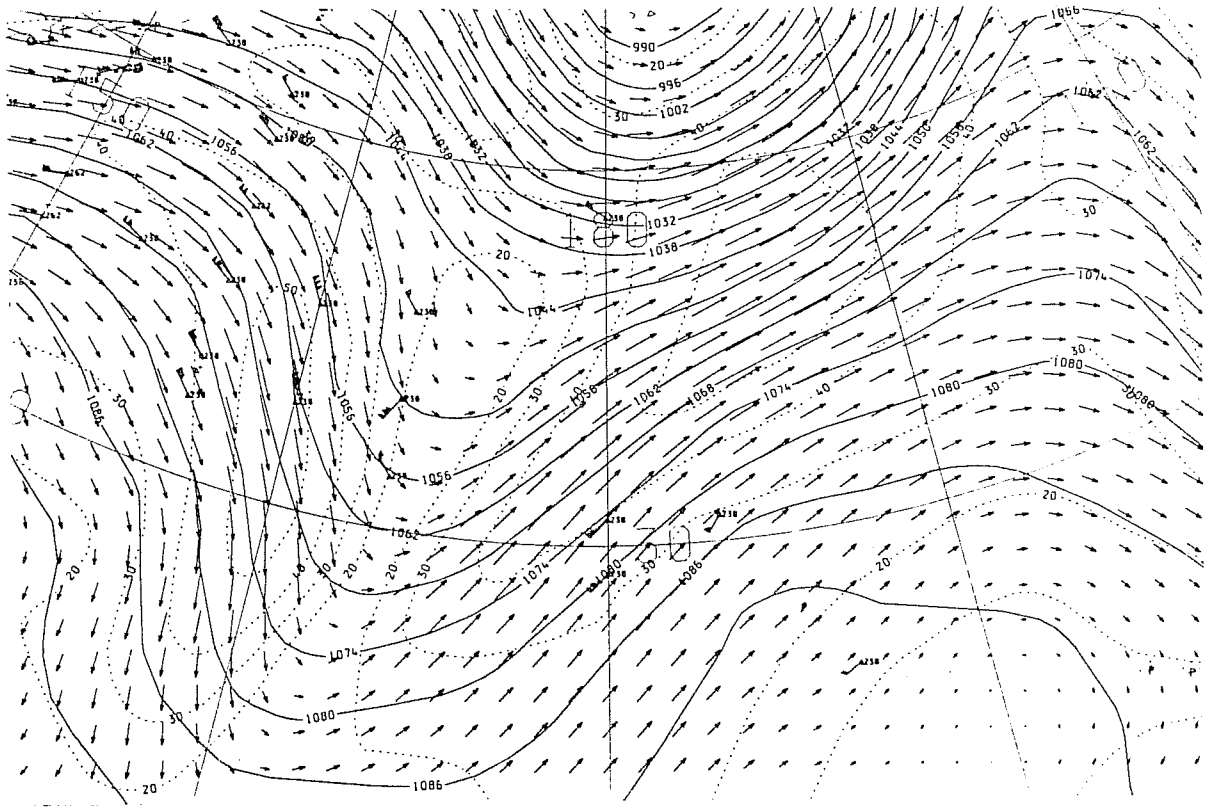

Figure 7. 6 hour forecast with UKMO model from ECMWF with-aircraft analysis.

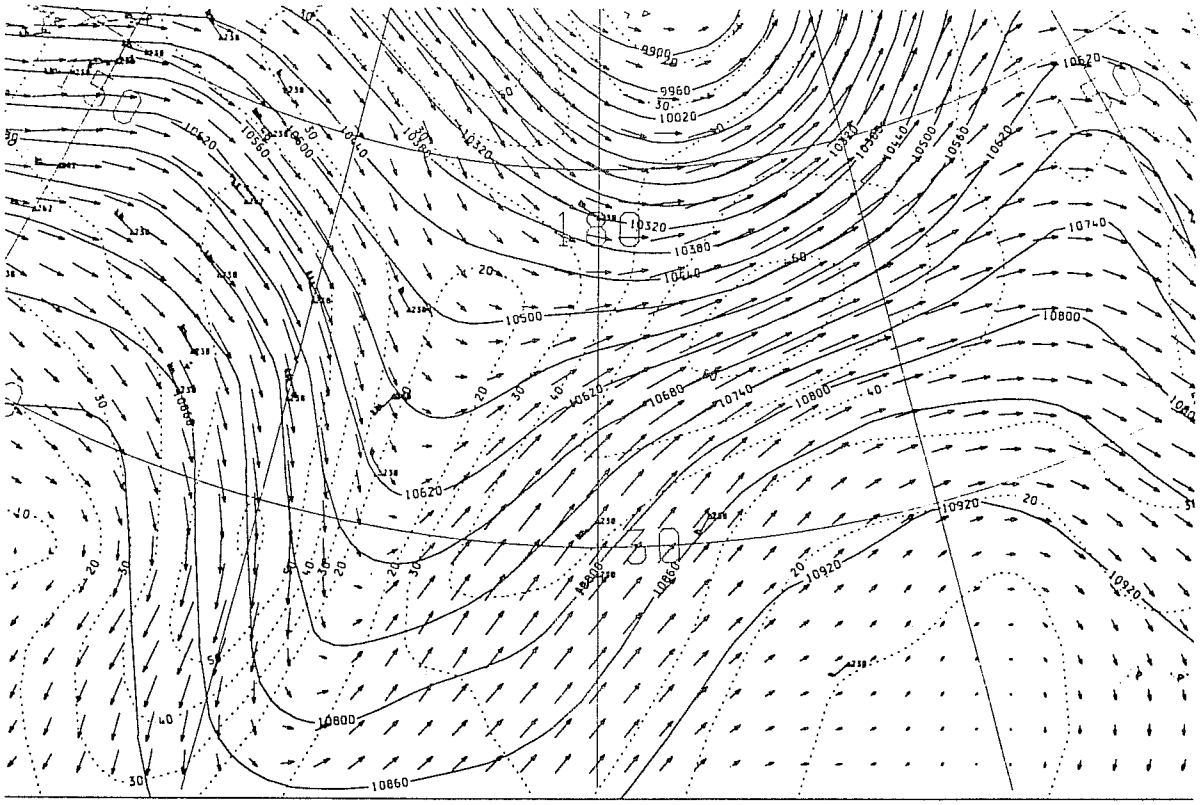

Figure 8. Verifying analysis for 6 hour forecasts.

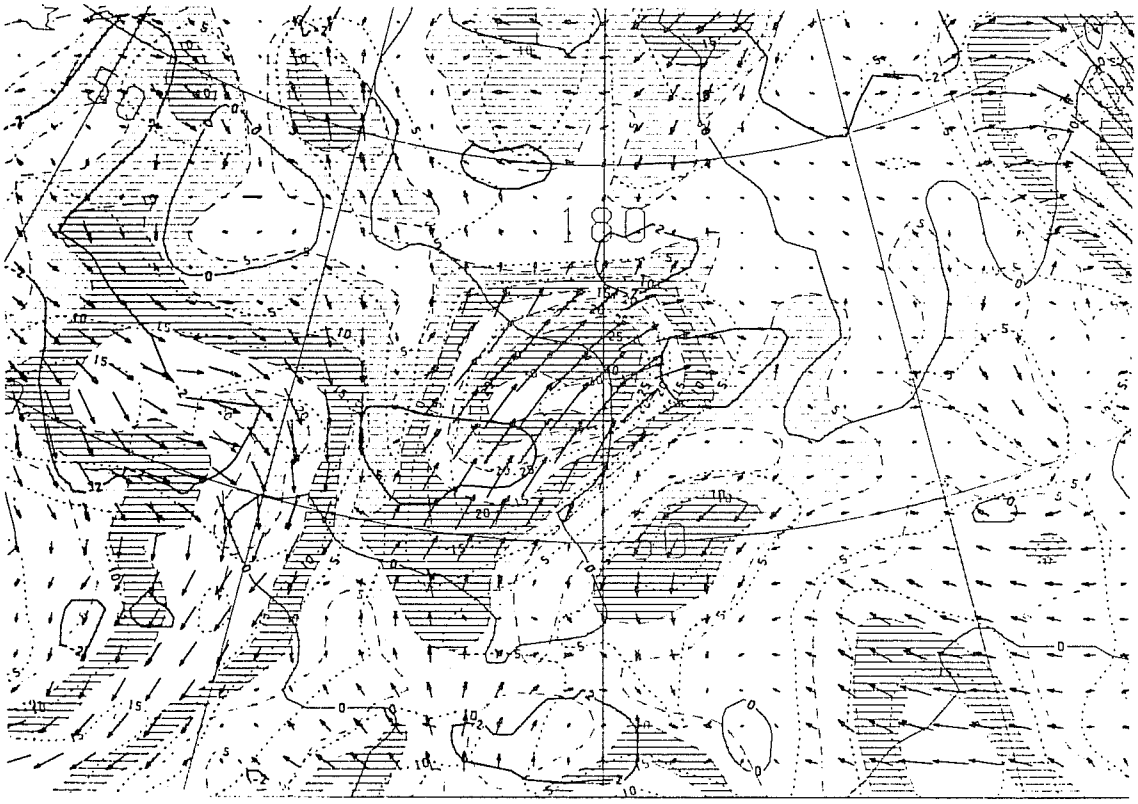

Figure 9. Difference between with- and without-aircraft analyses, with fainter arrows and shading showing ageostrophic component.

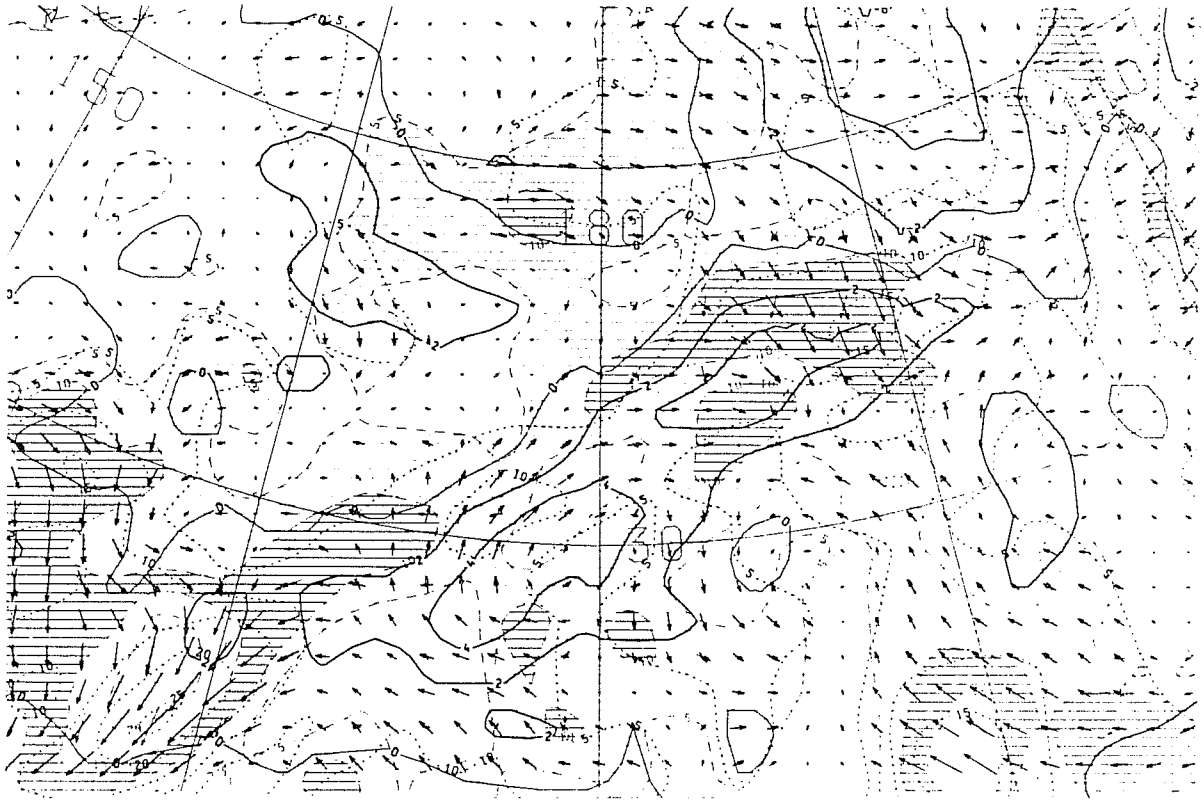

Figure 10 as Figure 9 for 6 hour forecast.

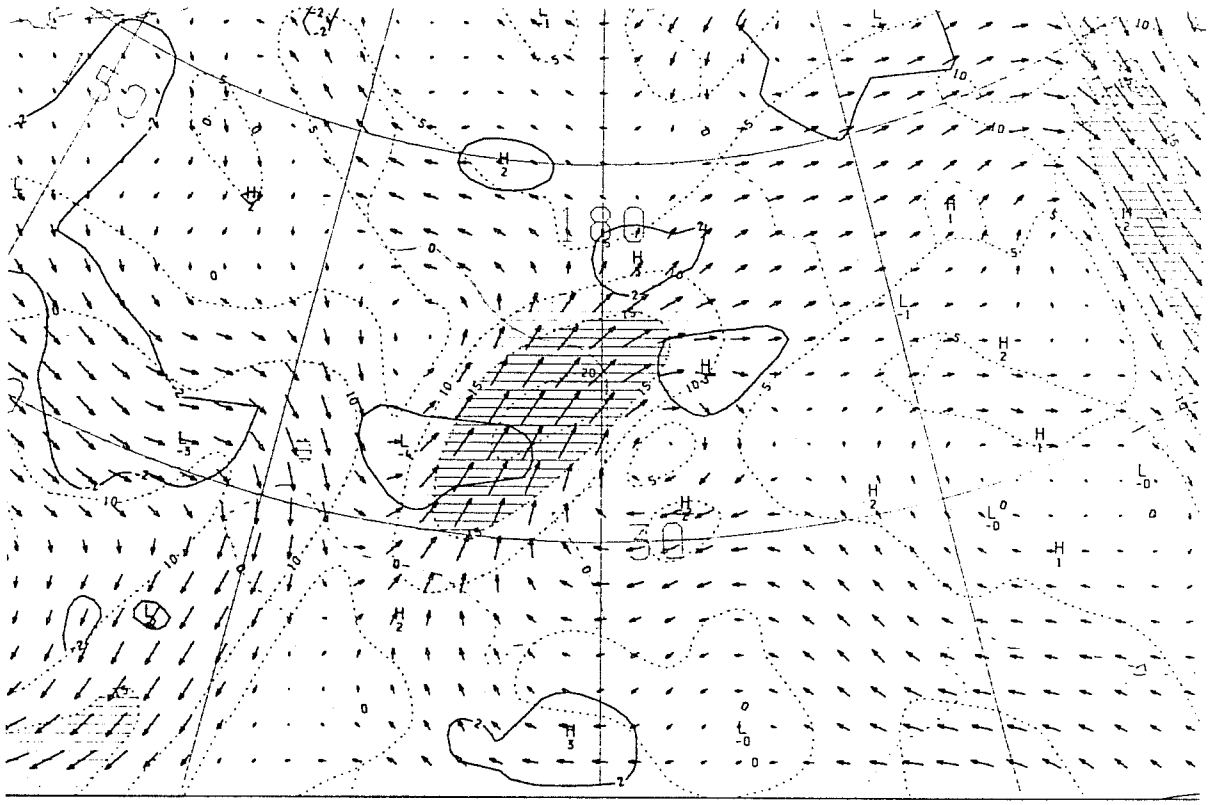

Figure 11. Rotational part of wind difference and height between with- and without-aircraft analyses.

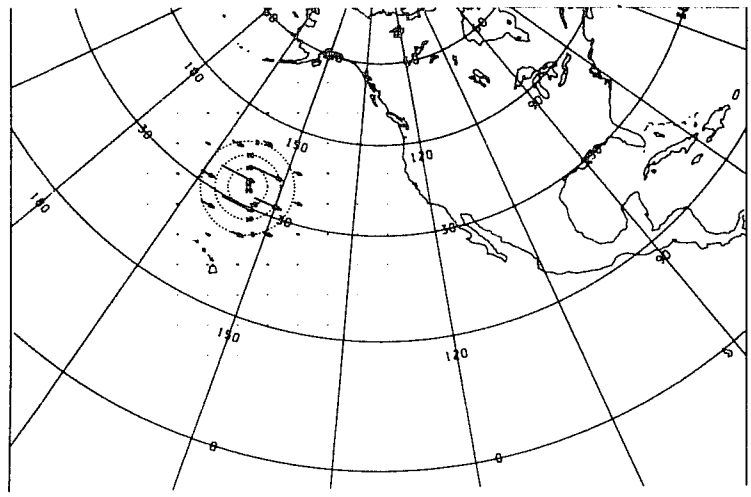

Figure 12. Wind perturbation at 232 mb (max speed 20 m/s).

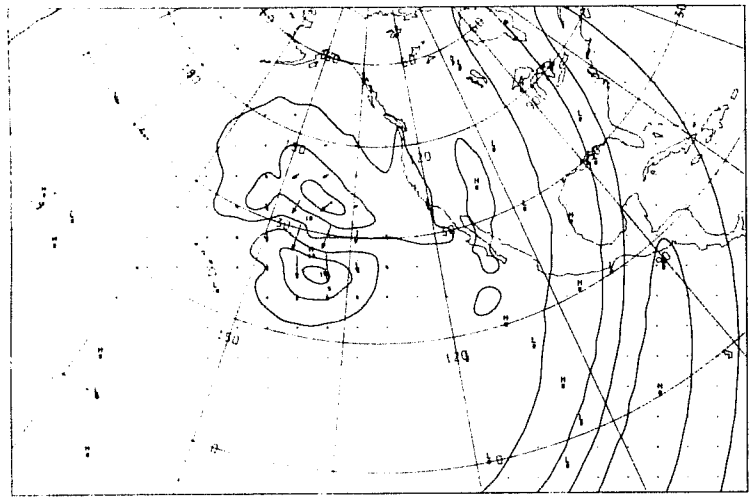

Figure 13. 6 hour forecast difference at 232 mb caused by single level wind perturbation. (contour interval 4 m, max speed 13 m/s).

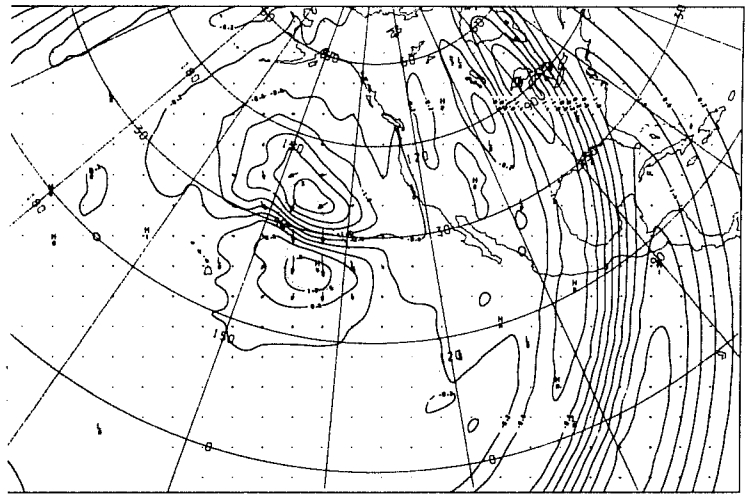

Figure 14. 6 hour forecast difference at 232 mb caused by multi-level wind perturbation. (contour interval 4 m, max speed 9 m/s).

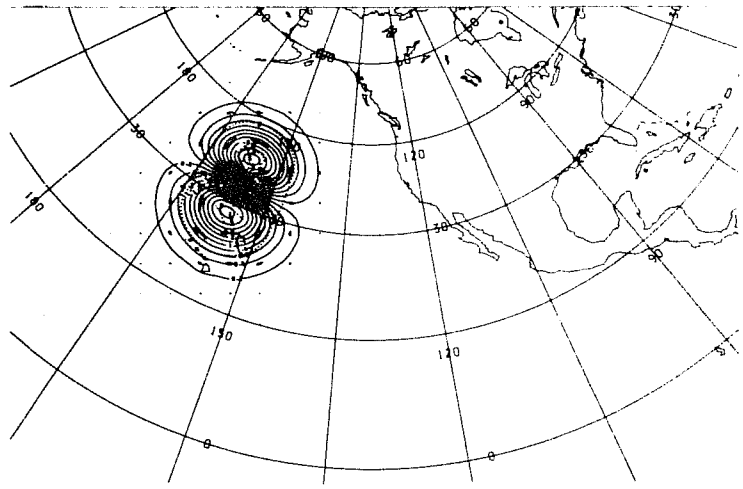

Figure 15. Non-divergent wind perturbation at 232 mb, and associated geostrophic height perturbation. (contour interval 4 m, max speed 20 m/s).

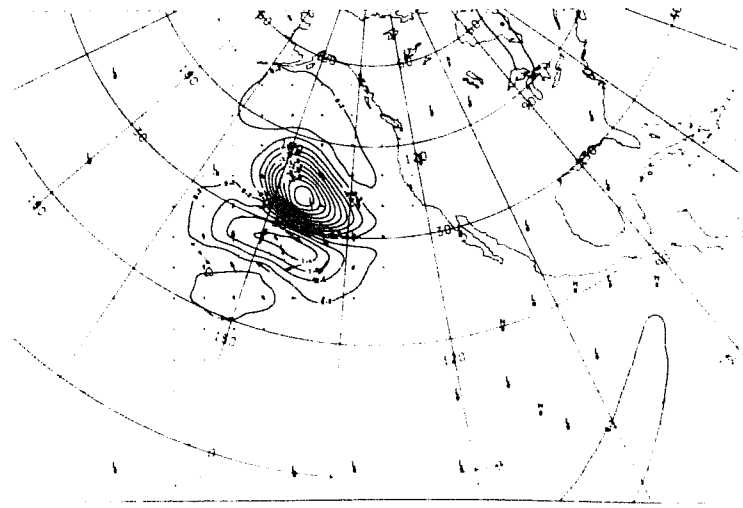

Figure 16. 6 hour forecast difference at 232 mb caused by multi-level non-divergent wind perturbation. (contour interval 4 m, max speed 12 m/s).

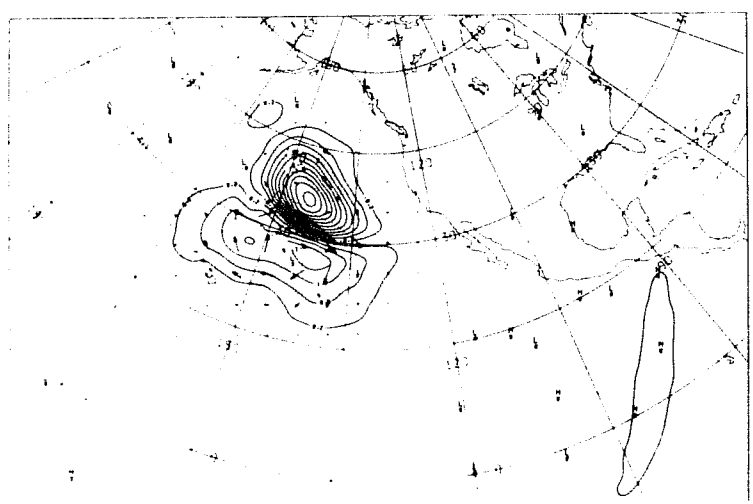

Figure 17. 6 hour forecast difference at 232 mb caused by multi-level non-divergent wind perturbation and geostrophic mass field perturbation. (contour interval 4 m, max speed 15 m/s).

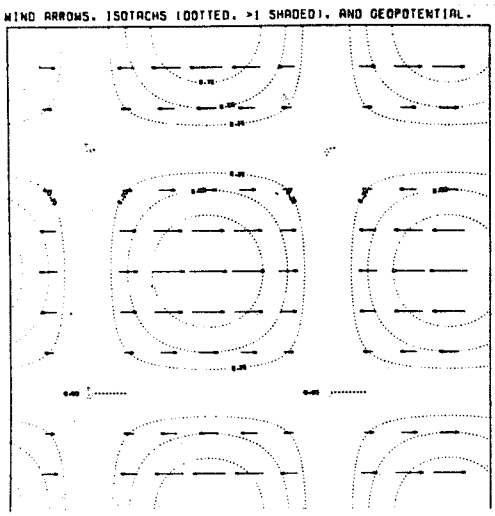

Figure 18. Wind perturbation.

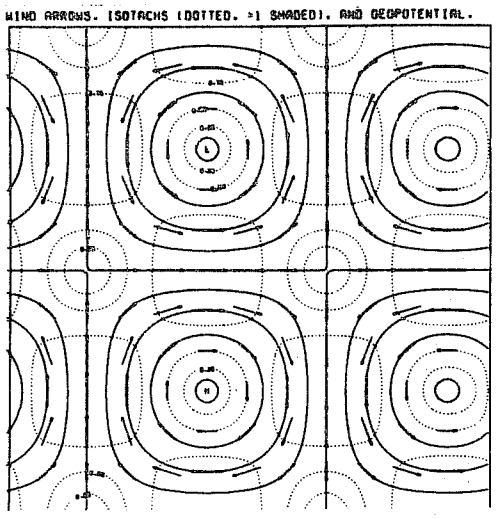

Figure 21. Non-divergent wind perturbation, with corresponding height perturbation.

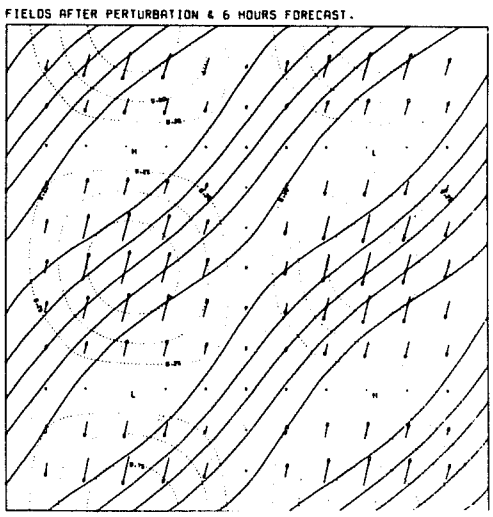

Figure 19. 6 hour forecast with 10 m equivalent depth from figure 18.

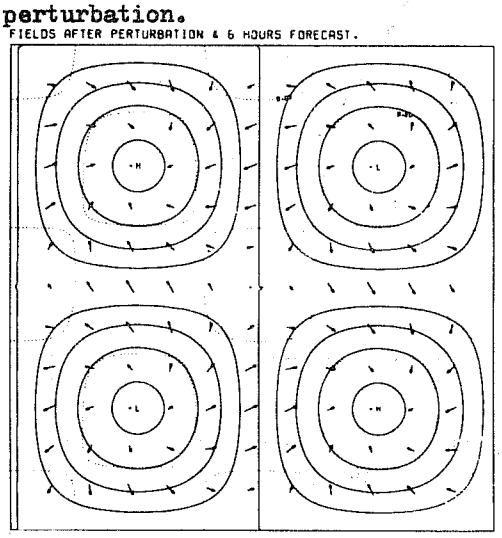

Figure 22. 6 hour forecast from non-divergent wind perturbation, 100 m equivalent depth.

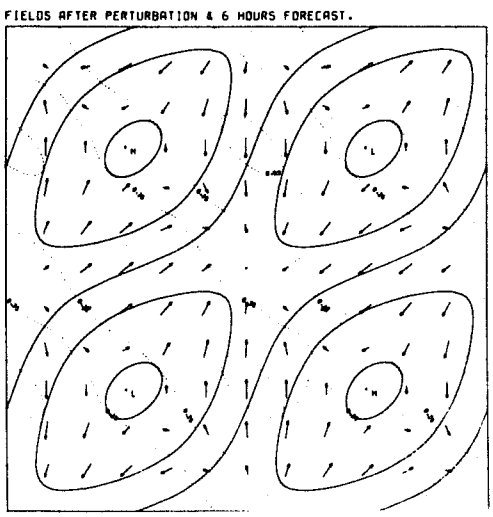

Figure 20. 6 hour forecast with 100 m equivalent depth from figure 18.

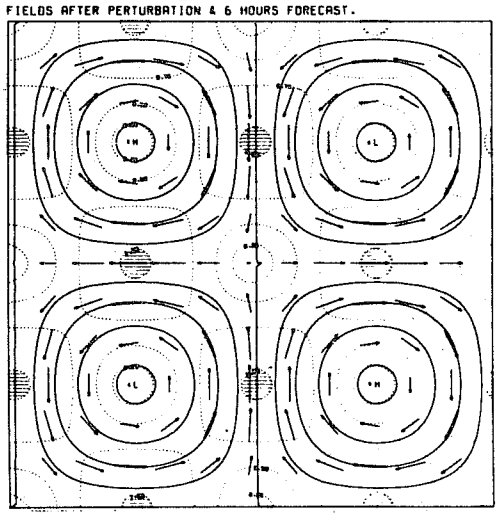

Figure 23. 6 hour forecast from geostrophic height and wind perturbation.

Figures 18–23. Fields from linear single wavelength shallow water equation model, simulating figures 12–17. Latitude 33°N, wavelength 3142 km, isotachs dotted at intervals of .25 initial perturbation, advective velocity 50 m/s.

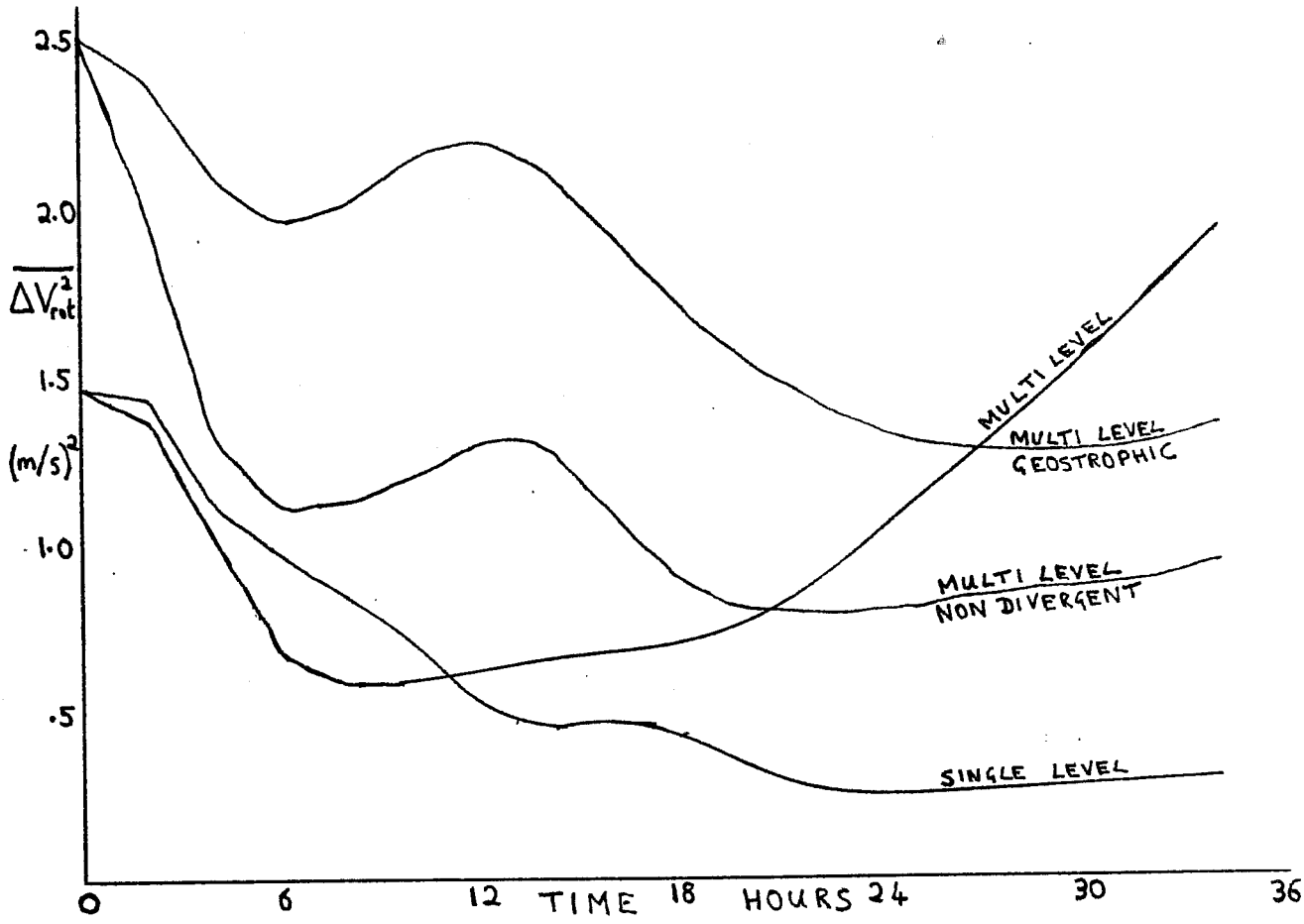

Figure 24. Mean square rotational component of wind difference at 232 mb for the area of figures 12–17, for the four perturbation experiments.

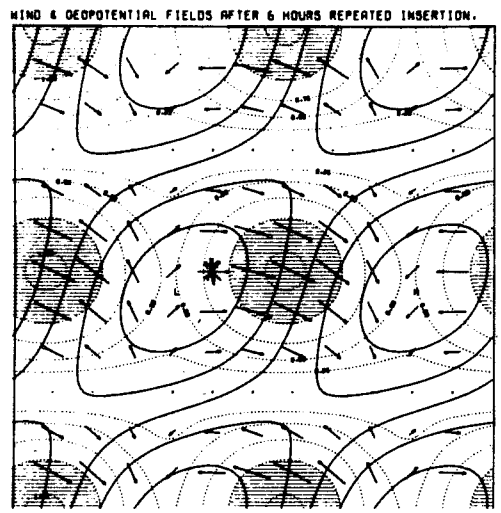

Figure 25. Height and wind field after 6 hours univariate repeated insertion, equivalent depth 10 m, other parameters as figures 18–23. * marks observation position. Speed greater than observed shaded. (compare figure 9).

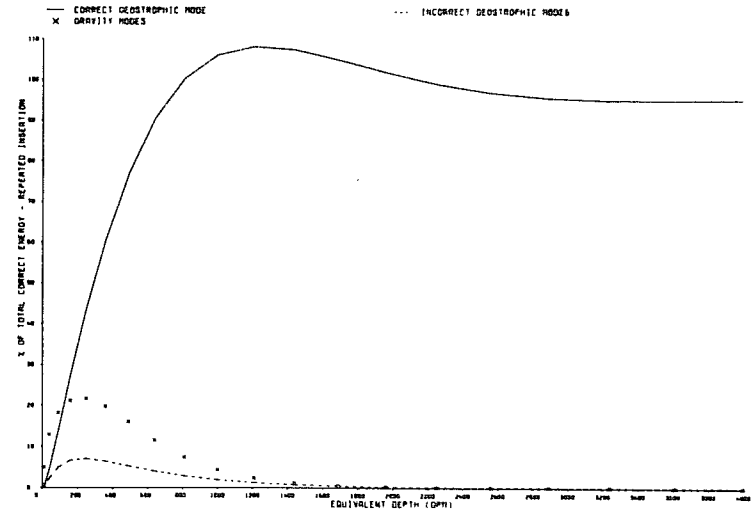

Figure 26. Energies in each mode as function of equivalent depth after univariate repeated insertion.

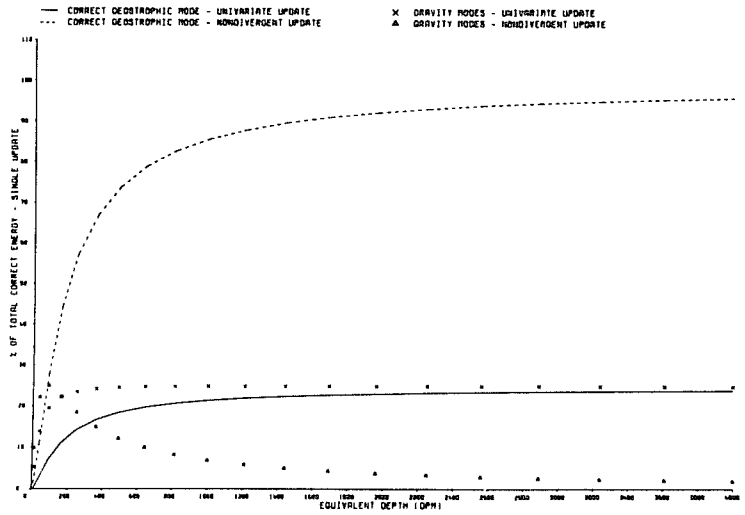

Figure 27. Energies in each mode as function of equivalent depth after perturbation with winds of figure 18 (solid line and X) and figure 21 (dashed line and Δ).

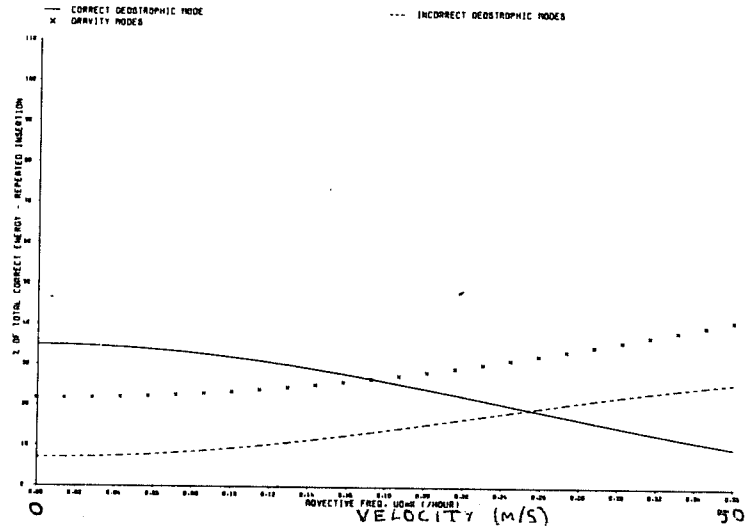

Figure 28. Energies in each mode as function of advective velocity after univariate repeated insertion, equivalent depth 200 m.